Supplement of The Cryosphere, 19, 6989–7012, 2025
https://doi.org/10.5194/tc-19-6989-2025-supplement


The Cryosphere
Open Access

*Supplement of*

# Global climate system response to SOFIA Antarctic meltwater in HadCM3-M2.1

**Amar Mistry et al.**

*Correspondence to:* Amar Mistry (amar.mistry.2018@bristol.ac.uk)

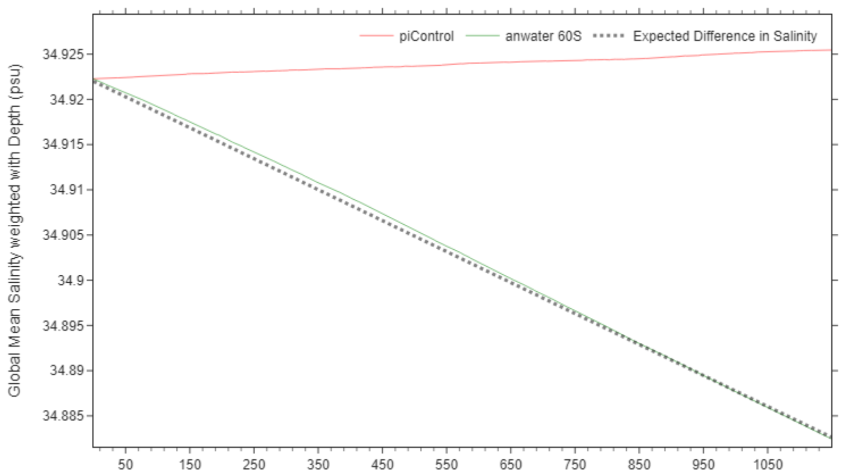


**Fig. S1.** Annual mean global salinity weighted with depth (psu) time series for piControl (red) and antwater 60S (green). Dashed grey line shows expected changes in global salinity weighted with depth based on projected input of freshwater.

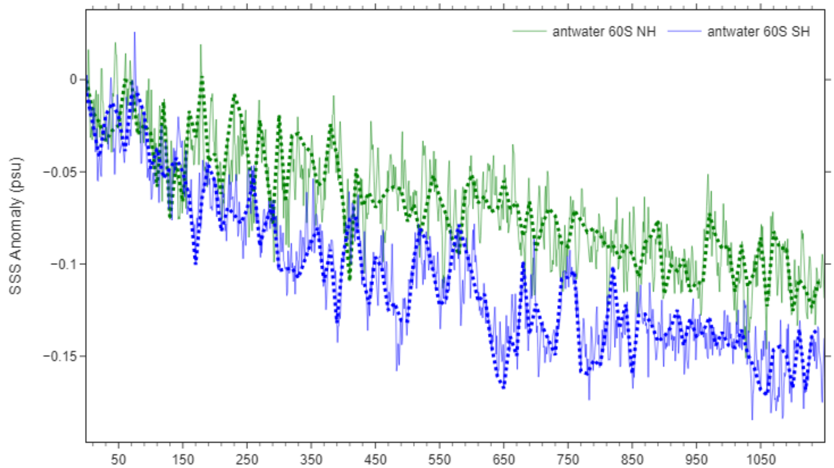


**Fig. S2.** Annual mean SSS (psu) anomaly time series by hemisphere for antwater 60S. NH and SH are shown in green and blue respectively. Dashed lines show ensemble means smoothed with a 10-yr running average.

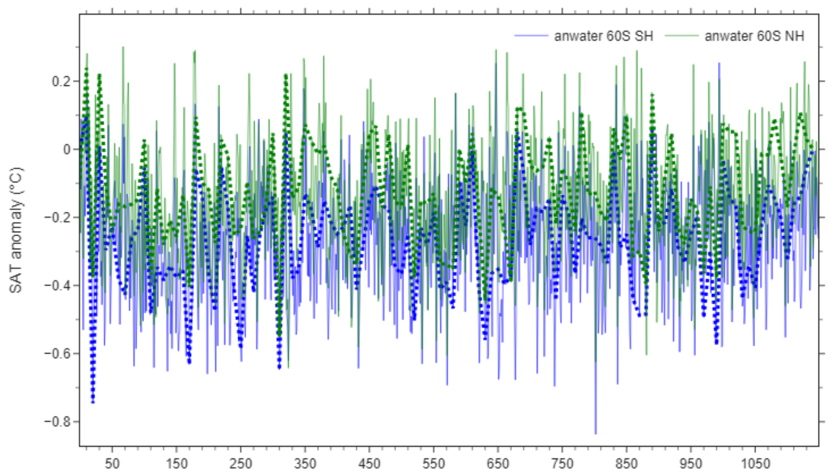


**Fig. S3.** Annual mean SAT (°C) anomaly time series by hemisphere for antwater 60S. NH and SH are shown in green and blue respectively. Dashed lines show ensemble means smoothed with a 10-yr running average.

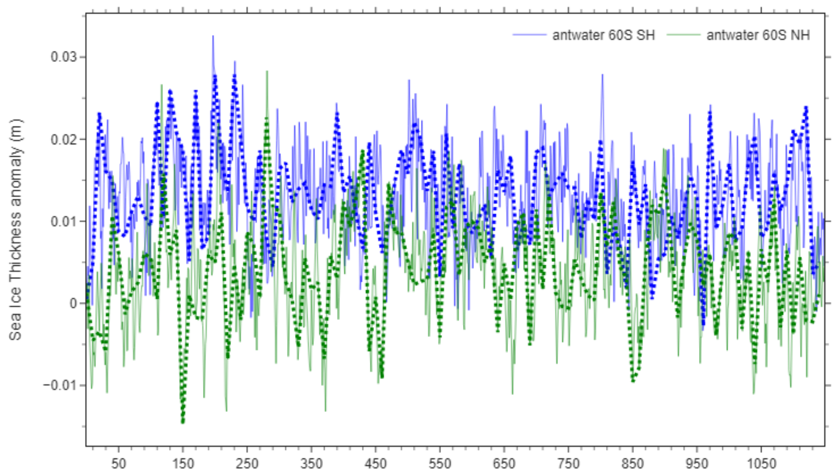


**Fig. S4.** Annual mean sea ice thickness (m) anomaly time series by hemisphere for antwater 60S. NH and SH are shown in green and blue respectively. Dashed lines show ensemble means smoothed with a 10-yr running average.

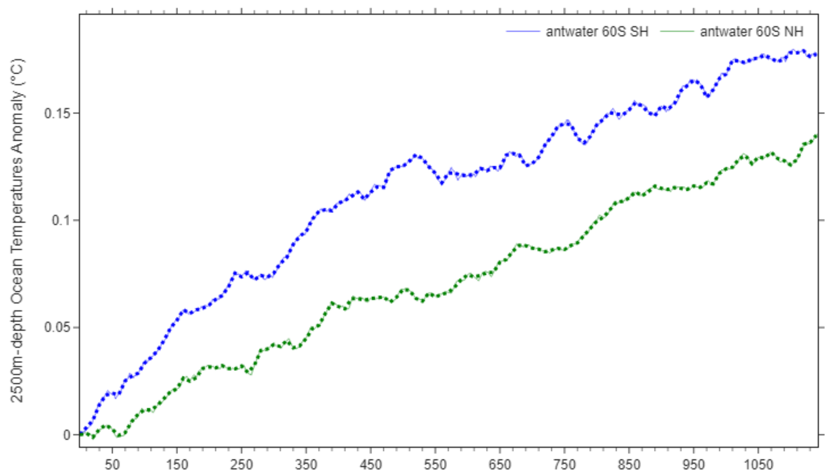


**Fig. S5.** Annual mean subsurface temperatures at 2500m (°C) anomaly time series by hemisphere for antwater 60S. NH and SH are shown in green and blue respectively. Dashed lines show ensemble means smoothed with a 10-yr running average.

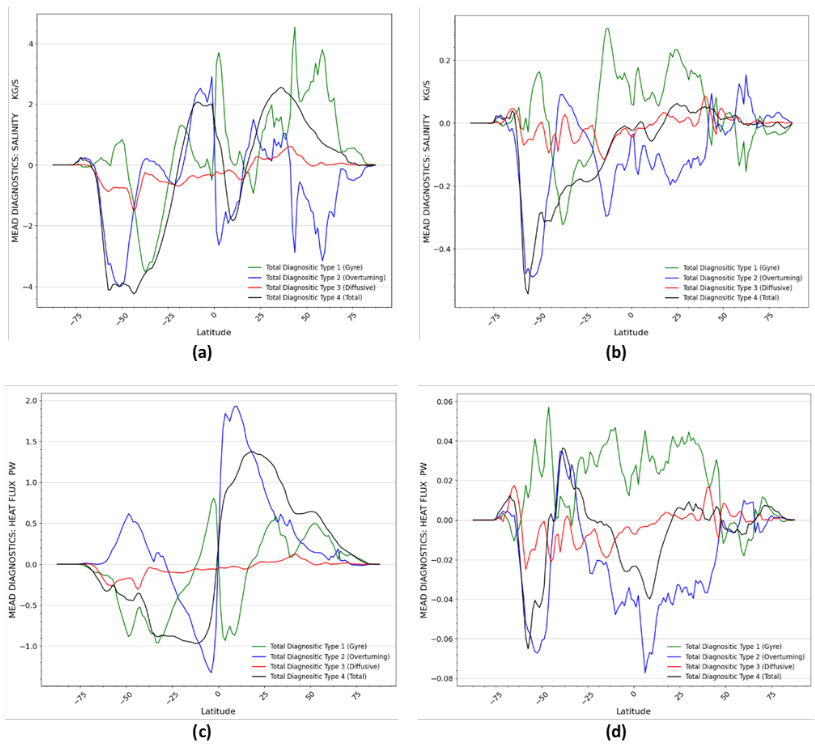


**Fig. S6.** (a) Salinity transport (kg/s) partitioned into type for antwater 60S in 950-1000. (b) Salinity transport anomaly (kg/s) partitioned into type for antwater 60S relative to piControl. (c-d) Same as above for northward heat transport (PW).

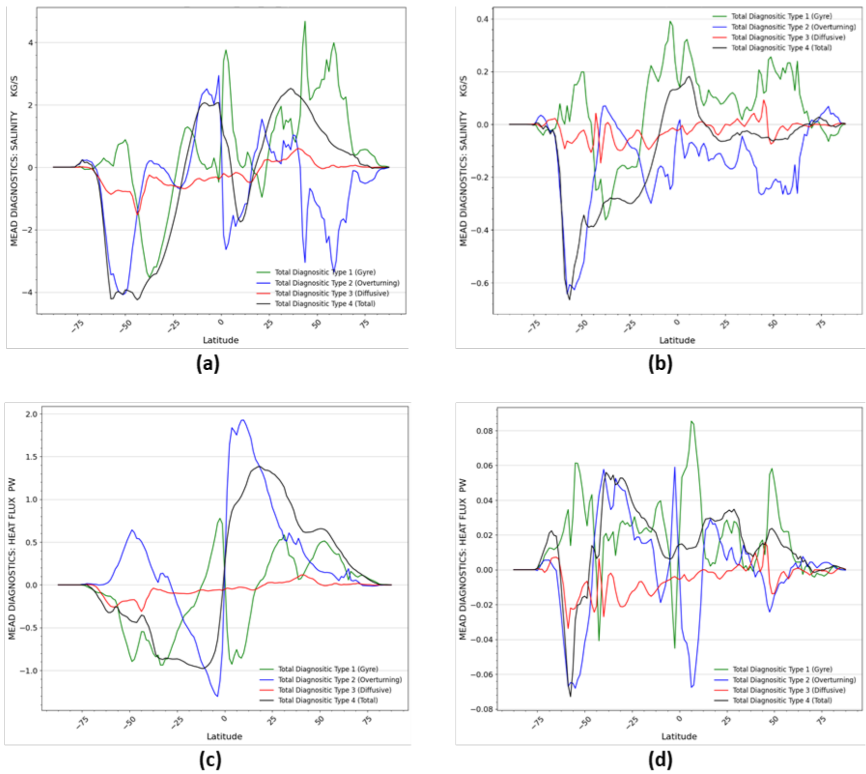


**Fig. S7.** (a) Salinity transport (kg/s) partitioned into type for antwater 60S in 1100-1150. (b) Salinity transport anomaly (kg/s) partitioned into type for antwater 60S relative to piControl. (c-d) Same as above for northward heat transport (PW).

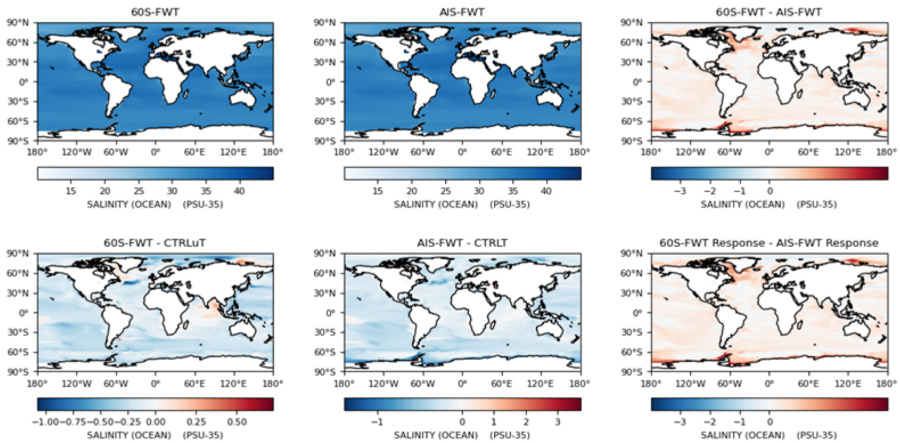


**Fig. S8.** 1100-1150 global SSS (psu) for antwater 60S and antwater, labelled accordingly. 1100-1150 anomalies in SSS (psu) for antwater 60S relative to antwater, antwater 60S relative to piControl, antwater relative to piControl and the antwater 60S response to meltwater relative to the antwater response, labelled accordingly.

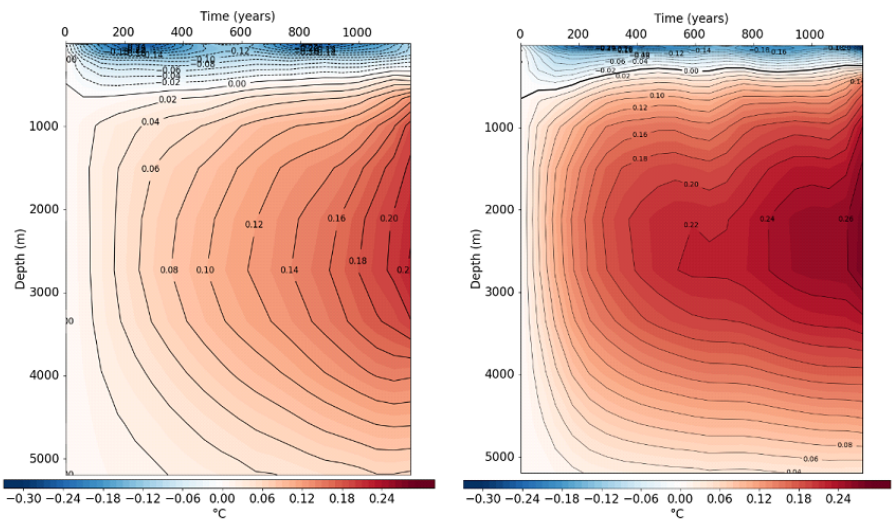


**Fig. S9.** (a) Hovmuller diagram (depth (m) vs time) of anomalous global ocean temperatures (°C) for antwater relative to piControl. (b) Hovmuller diagram of the anomalous SO temperatures (°C) for antwater relative to piControl. Solid black line represents the point at which the salinity anomaly changes from positive to negative

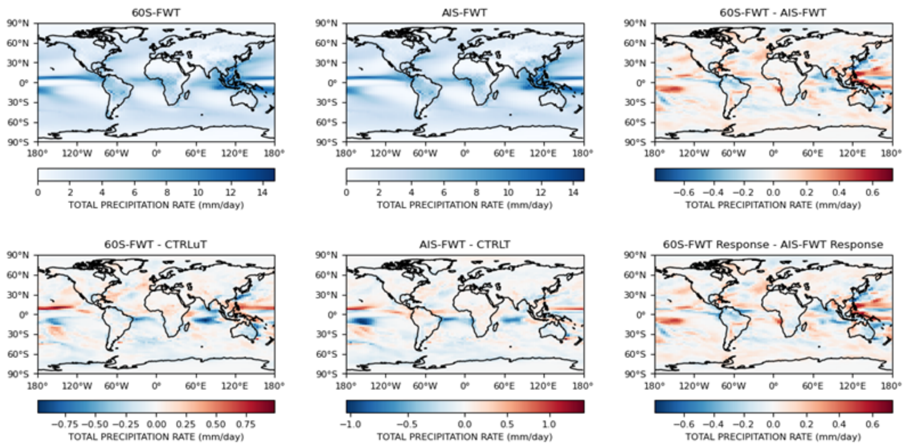


**Fig. S10.** 1100-1150 global precipitation (mm/day) for antwater 60S and antwater, labelled accordingly. 1100-1150 anomalies in global precipitation (mm/day) for antwater 60S relative to antwater, antwater 60S relative to piControl, antwater relative to piControl and the antwater 60S response to meltwater relative to the antwater response, labelled accordingly.

**Table S1.** Experiment design list for the SOFIA initiative (Swart et al., 2023).

| Name | Freshwater perturbation (Sv) | Branch year | Time span (year) | Additional forcings |
|---|---|---|---|---|
| Tier-1 | | | | |
| piControl | None | N/A | $\geq$ 100 | Fixed preindustrial |
| antwater | Fixed 0.1 | Model year | $\geq$ 100 | Fixed preindustrial |
| | | | | |
| Tier 2 | | | | |
| Hist-antwater-70-01 | Increasing by 0.1 ($x10^{-3}$ $Sv \cdot yr^{-1}$) | 1970 | 1970-2020 | Historical |
| Hist-antwater-70-03 | Increasing by 0.3 ($x10^{-3}$ $Sv \cdot yr^{-1}$) | 1970 | 1970-2020 | Historical |
| Hist-antwater-70-05 | Increasing by 0.5 ($x10^{-3}$ $Sv \cdot yr^{-1}$) | 1970 | 1970-2020 | Historical |
| Hist-antwater-92-11 | Increasing by 1.1 ($x10^{-3}$ $Sv \cdot yr^{-1}$) | 1992 | 1992-2020 | Historical |
| | | | | |
| ssp126-ismip6-water | Fixed 0.015 | 2015 | 2015-2100 | SSP126 scenario |
| ssp585-ismip6-water | Increased nonlinearly; Maximum 0.196 | 2015 | 2015-2100 | SSP585 scenario |
| | | | | |
| Tier 3 | | | | |
| 60S water | Fixed 0.1[a] | Model year | $\geq$ 100 | Fixed preindustrial |
| antwater-lh | Fixed 0.1[b] | Model year | $\geq$ 100 | Fixed preindustrial |
| Antwater-ambe | Fixed 0.1[c] | Model year | $\geq$ 100 | Fixed preindustrial |
| Antwater-depth | Fixed 0.1[d] | Model year | $\geq$ 100 | Fixed preindustrial |
| Antwater-depth-lh | Fixed 0.1[b, d] | Model year | $\geq$ 100 | Fixed preindustrial |
| Antwater-ambe-depth-lh | Fixed 0.1[b, c, d] | Model year | $\geq$ 100 | Fixed preindustrial |

[a] Freshwater added south of 60 S. [b] Ocean cooling imposed to extract latent heat required to melt equivalent freshwater. [c] Freshwater added exclusively to the Amundsen and Bellingshausen seas (210° to 290° E). [d] Freshwater added uniformly from the surface to the continental shelf base.

Table S2: Survey of recent studies inserting freshwater forcing around the AIS into coupled or ocean-only models, including a brief description of their experiment designs. Model refers to atmosphere–ocean coupled (C), intermediate-complexity (I), or ocean-only (O) models. Function is the freshwater forcing function with time, either constant (C), linear (L), exponential (E), or variable (V). Depth is the depth of freshwater input being at the surface (S; < 50 m), with a uniform distribution (U) or a realistic distribution (R). Freshwater Input Duration refers to how long the experiments are run for in years.

| **Study** | **Model** | **Function** | **Depth (m)** | **Freshwater Input Duration (years)** | **Experiment Description** |
|---|---|---|---|---|---|
| Sadai *et al.,* (2020) | C | V | S | 245 | 2 sets of experiments; a) under a RCP4.5 scenario freshwater input increases until it peaks at 0.4-0.8 Sv; b) under a RCP8.5 scenario freshwater input increases until it peaks at >2 Sv ~125 years into the simulation |
| Golledge *et al.,* (2019) | C | V | S | 240 | 2 sets of experiments; freshwater input increases until it peaks at; 0.042 Sv and 0.015 Sv for Antarctica and Greenland, respectively, under RCP4.5; and 0.16 Sv and 0.018 Sv under RCP8.5. Freshwater is distributed in the North Atlantic, Ross and Weddell Seas |
| Purich and England, (2023) | C | L | S | 100 | 3 sets of experiments; freshwater input increases to a) 0.18 Sv (5600 Gt yr$^{-1}$); b) 0.55 Sv (17350 Gt yr$^{-1}$); c) 0.45 Sv (14300 Gt yr$^{-1}$) |
| Bronselaer *et al.,* (2018) | C | V | S | 150 | Freshwater injection that increases non-linearly to 0.6 Sv added around the Antarctic coast under RCP8.5 scenario |
| Hansen *et al.,* (2016) | C | E | S | 300 | Freshwater injection of 360 Gt yr$^{-1}$ for an initial 12 years, then grows with 5-, 10- or 20-year doubling time and terminates when global sea level reaches 1 or 5 m. |
| Ma, Wu and Li, (2013) | C | C | S | 400 | 1Sv freshwater is added uniformly south of 60°S |
| Stouffer, Seidov and Haupt, (2007) | C | C | S | 200 | 1Sv freshwater is added uniformly south of 60°S for 100 years and then removed |
| Mackie *et al.,* (2020) | C | E | R | 100 | Freshwater injection across the SO increases by 2.33% yr$^{-1}$ |
| van den Berk and Drijfhout, (2014) | C | E | S | 104 | Freshwater injection that increases to a peak of ~5050 Gt yr$^{-1}$ and ~2200 Gt yr$^{-1}$ at areas of observed mass loss around AIS and Greenland, respectively, under a RCP8.5 scenario |
| Li, Marshall, *et al.,* (2023) | C | C | U | 50 to 100 | 9 experiments; 500 Gt yr$^{-1}$, 2000 Gt yr$^{-1}$ and 5000 Gt yr$^{-1}$ applied along the coast of Greenland, Antarctica and both |
| Fogwill *et al.,* (2015) | C | C | S | 200 to 1000 | Initial 0.069 Sv freshwater flux delivered into Amundsen Sea embayment for 200 years, followed by additional freshwater flux into Ross and Weddell Sea sectors over up to 900 years |
| Pauling *et al.,* (2017) | C | L | R | 33 | Freshwater injection that increases linearly to 4000 Gt yr$^{-1}$ |

| | | | | | |
|---|---|---|---|---|---|
| Beadling *et al.*, (2022) | C | C | S | 70 | 0.1 Sv freshwater is added in a one-degree latitude band in regions of observed ice shelf and ice sheet melt |
| Bronselaer *et al.*, (2020) | C | C | S | 95 | 0.02 Sv freshwater is added around the Antarctic coast |
| Park and Latiff, (2019) | C | C | S | 200 | 3 experiments where 0.1 Sv and 0.05 Sv freshwater is added around the Antarctic coast, and 0.02Sv freshwater is added around WAIS |
| Rye *et al.*, (2020) | C | V | U | 30 | Pre-industrial state that is perturbed by an abrupt 200 Gt $yr^{-1}$ step increase in freshwater flux |
| Bintanja *et al.*, (2013) | C | C | S | 31 | 250 Gt $yr^{-1}$ freshwater is added around the Antarctic coast |
| Pauling *et al.*, (2016) | C | C | R | 33 | 2 sets of experiments; a) 1000, 2000 and 3000 Gt $yr^{-1}$ freshwater is added around the Antarctic coast; b) 167 and 2000 Gt $yr^{-1}$ freshwater is added around Antarctic ice shelf fronts |
| Bintanja, Oldenborgh and Katsman, (2015) | C | C | S | 40 | 10, 20, 60 and 120 Gt $yr^{-1}$ is added around the Antarctic coast under RCP8.5 scenario |

| | | | | | |
|---|---|---|---|---|---|
| Swingedouw *et al.*, (2009) | I | C | S | 600 | 2 sets of experiments; a) 1 Sv is added south of 60°S for 100 years and then removed; b) 2Sv for 50 years and then removed |
| Weaver *et al.*, (2003) | I | L | S | 500 | 2 sets of experiments; a) freshwater is added around the southern tip of South America, increasing to 1 Sv; b) same freshwater perturbation is added west of Antarctic Peninsula |
| Aiken and England, (2008) | I | C | S | 400 | 4 sets of experiments; 0.004 Sv freshwater is added to all sea-ice covered grid boxes in the southern Hemisphere for a) 1 and b) 100 years; c) 0.004 Sv is applied to Antarctic coast for 1 year; d) 0.4 Sv is applied to all sea-ice covered grid boxes in the southern hemisphere for 100 years |
| Menviel *et al.*, (2010) | I | C, L | S | 400 to 800 | 2 sets of experiments; a) 0.18 Sv and 0.35 Sv freshwater is added around WAIS for 800 and 400 years respectively; b) same as a) with additional atmospheric CO2 doubling over 100 years |
| Swart and Fyfe, (2013) | I | L | S | 31 | 2 sets of experiments; a) five different rates of mass loss acceleration; b) ten different rates of acceleration starting in 13 years. Two different distributions for each experiment; a) adjacent to Antarctic shelf; b) along coast of Amundsen Bay |

| | | | | | |
|---|---|---|---|---|---|
| Lago and England, (2019) | O | E | S | 200 | 3 sets of experiments based on freshwater inputs under RCP2.6, RCP4.5 and RCP8.5 calculated by DeConto and Pollard (2016) (REF). 2 different distributions for each experiment; a) along Antarctic coast; b) includes freshwater from iceberg melt estimates |
| Moorman, Morrison and Hogg, (2020) | O | C | S | 10 | 0.042 Sv and 0.16 Sv freshwater is added around regions of high mass loss rates |
| Li, England, *et al.,* (2023) | O | L | S | 49 | Freshwater injection that increases to 0.009 Sv and 0.080 Sv along coast of Greenland and WAIS, respectively, under a RCP8.5 scenario |
| Merino *et al.,* (2018) | O | C | R | 31 | <0.01 Sv (282 Gt $yr^{-1}$) freshwater is added along the ice shelf front |
| Seidov, Barron and Haupt, (2001) | O | C | S | 2000 | Series of 14 experiments adding freshwater in the range of 0.002 to 0.087Sv to the North Atlantic, along the Antarctic coast and/or the Weddell Sea |
| Haumann, Gruber and Münnich, (2020) | O | C | U | 40 | 2 sets of experiments; freshwater input based on meltwater fluxes observed a) between 1982-2008 added south of 60°S; b) between 1992-2009 added 175°E to 75°W |

**Table S3.** List of model parameters varied with tuning according to Table 3.1 and Table 3.2 from Ross (2023), including the values pre and post tuning, and a brief description of the impacts. Model parameters are separated based on the tuning approach taken.

| Parameter description | Range of values | Value pre-tuning (uT) | Value post-tuning (T) | Expected impact of tuning |
|---|---|---|---|---|
| Objective Tuning | | | | |
| Relative humidity for cloud formation | 0.6 - 0.9 | 0.700 | 0.605 | More cloud forms under the same humidity (Irvine et al., 2013). |
| Lateral entrainment coefficient | 0.6 - 9.0 | 3.000 | 2.789 | This parameter controls the mixing of deep convective plumes with their surroundings. Thus, more air convecting clouds can be drawn in from surrounding grid boxes (Irvine et al., 2013; Ross, 2023). |
| Cloud droplet to rain conversion rate (s$^{-1}$) | $5.0e^{-5}$ - $4.0e^{-4}$ | $1.000e^{-4}$ | $2.690e^{-4}$ | Conversion of cloud water droplets to rain increases and cloud lifespan decreases (Rougier et al. 2009; Irvine et al 2013; Ross, 2023). |
| Threshold of liquid water for the formation of precipitation (over sea) (kg/m$^3$) | $2.0e^{-5}$ - $5.0e^{-4}$ | $5.000e^{-5}$ | $3.532e^{-5}$ | |
| Threshold of liquid water for the formation of precipitation (over land) (kg/m$^3$) | $1.0e^{-4}$ - $2.0e^{-3}$ | $2.000e^{-4}$ | $1.606e^{-4}$ | |
| Minimum albedo of sea ice | 0.47 - 0.65 | 0.50 | 0.61 | Albedo driven feedbacks increase but are less important in warmer climates (Ross, 2023). |
| Background coefficient of vertical mixing of momentum | - | $1.000e^{-5}$ | $1.419e^{-5}$ | Stronger oceanic overturning and deep water formation increases (Ross, 2023). |
| Vertical diffusion rate of increase with depth (m/s) | - | $2.800e^{-8}$ | $5.638e^{-8}$ | |
| Ice-fall speed (m/s) | 0.5 - 2.0 | 1.000 | 1.339 | Ice particle size increases, associated with decreases in cirrus cloud coverage, longwave cloud forcing and upper troposphere water vapour (Sanderson et al.; Mitchell et al., 2011). |
| Subjective tuning | | | | |
| Cloud drop number (land) (drop/cm$^3$) | - | 125 | 50 | Precipitation rate increases, cloud lifetime becomes shorter and cloud cover reduces (Kiehl and Shields, 2013). |
| Cloud drop number (sea) | - | 70 | 50 | |
| Cloud drop radii (land) (um) | - | 13.500 | 17.000 | |
| Cloud drop radii (sea) (um) | - | 17.000 | 17.000 | |
| Other | | | | |
| Solar constant (W/m$^2$) | - | 1365 | 1361 | Change made to be consistent with CMIP6 protocols. |